

# On the ability of various circular inspiral templates that incorporate radiation reaction effects at the second post-Newtonian order to capture inspiral gravitational waves from compact binaries having tiny orbital eccentricities

Manuel Tessmer\* and Achamveedu Gopakumar†

*Theoretisch-Physikalisches Institut, Friedrich-Schiller-Universität Jena, Max-Wien-Platz 1, 07743 Jena, Germany*

(Dated: February 7, 2022)

We probe the ability of various types of post-Newtonian(PN)-accurate circular templates to capture inspiral gravitational-wave (GW) signals from compact binaries having tiny orbital eccentricities. The GW signals are constructed by adapting the phasing formalism, available in T. Damour, A. Gopakumar, and B. R. Iyer, [Phys. Rev. D **70**, 064028 (2004)]. And, we employ the orbital energy and the time-eccentricity to describe the orbital evolution of eccentric binaries that incorporate the 3PN-accurate conservative and the 2PN-accurate reactive dynamics. Using the fitting factor estimates, relevant for the initial LIGO, we show that circular templates, based on the adiabatic TaylorT1, complete adiabatic TaylorT1 and TaylorT4 approximants, that require the 2PN-accurate energy flux are unable to capture our GW signals from compact binaries having tiny residual orbital eccentricities. However, the 2PN-order circular inspiral templates based on the recently introduced TaylorEt approximant are found to be both *effectual* and *faithful* in capturing GWs from inspiralling compact binaries having moderate eccentricities and we provide physical explanations for our observations. We conclude that further investigations involving the actual interferometric data may be required to probe the ability of the widely employed traditional 2PN order circular templates to capture inspiral GWs from astrophysical compact binaries, like the plausible compact binary progenitor candidate for the GRB 070201, that are expected to contain tiny residual orbital eccentricities.

PACS numbers: 04.30.Db, 04.25.Nx 04.80.Nn, 97.60.Jd, 95.55Ym

## I. INTRODUCTION

Inspiral GWs from non-spinning stellar mass compact binaries are being searched in the data generated by the operational first generation ground-based laser interferometric GW detectors [1]. The GW data analysts employ the technique of *matched filtering* [2] that demands theoretically modeled inspiral templates to extract astrophysical GW signals from the noisy interferometric data. The theoretical inspiral templates require the temporally evolving GW polarizations  $h_+(t)$  and  $h_\times(t)$ , and are usually constructed by employing the PN approximation to general relativity. In the case of inspiralling compact binaries, usually modeled to consist of point masses, the PN approximation provides, for example, the orbital dynamics as corrections to the Newtonian equations of motion in terms of  $(v/c)^2 \sim Gm/c^2 r$ , where  $v$ ,  $m$  and  $r$  are the characteristic orbital velocity, the total mass, and the typical orbital separation, respectively.

The LIGO Scientific Collaboration (LSC) [3] employs various types of PN-accurate inspiral templates, detailed in Ref. [4], for analyzing the LIGO data for inspiral GWs. These templates are constructed by keeping only the Newtonian contributions to the amplitudes of  $h_+(t)$  and  $h_\times(t)$ , while their phase evolutions are PN-accurate, resulting in the so-called restricted PN waveforms. While searching for inspiral GW signals from non-spinning com-

pact binaries, it turned out that the LSC had invoked various types of restricted 2PN order waveforms [5]. These inspiral template families provide slightly different prescriptions for the GW phase evolution that incorporate gravitational radiation reaction (RR) effects at the 2PN order, *i.e.*,  $(v/c)^4$  corrections beyond the Newtonian (quadrupolar) RR order. These templates represent gravitational radiation field generated by compact binaries inspiralling under the action of 2PN-accurate RR effects along circular orbits. The approximation of quasi-circularity, namely inspiral along a sequence of circular orbits, is justified due to the fact that the gravitational RR forces are highly efficient in circularizing orbits of compact binaries [6].

Interestingly, the ability of the 2PN-accurate circular templates, available in Ref. [4], to detect GWs from compact binaries in inspiralling eccentric orbits is not explored in the literature and we speculate that it may be due to Ref. [7]. With the help of GW signals associated with compact binaries moving in Newtonian-accurate eccentric orbits and inspiralling under quadrupolar RR order, Ref. [7] demonstrated that the Newtonian order circular templates are quite efficient in extracting even their mildly eccentric GW signals. However, we recently pointed out that the arguments presented in Ref. [7] should not be used to support the ability of the traditional PN-accurate circular templates to capture inspiral GWs from compact binaries having tiny orbital eccentricities [8]. This is because in Ref. [8], we demonstrated that the three types of circular inspiral templates based on the adiabatic, complete adiabatic and gauge-dependent completely non-adiabatic approximants, detailed in Ref. [9]

\*Electronic address: M.Tessmer@uni-jena.de

†Electronic address: A.Gopakumar@uni-jena.de

and relevant for the circular inspiral under the quadrupolar RR order, are inefficient in capturing GWs from eccentric compact binaries having 2.5PN-accurate orbital evolution, detailed in Ref. [10]. The present paper extends the analysis presented in Ref. [8] by incorporating RR effects to 2PN (relative) order, while constructing both the GW signals and the circular search templates.

In this paper, we explore the ability of a number of PN-accurate circular templates, detailed in Refs. [4, 9, 11, 12], that employ the radiation reaction effects to the relative 2PN accuracy to capture GW signals from compact binaries in inspiralling eccentric orbits, constructed by adapting the phasing formalism, detailed in Ref. [10]. We construct GW signals by perturbing compact binaries moving in 3PN-accurate precessing eccentric orbits with RR effects that are 2PN-accurate, beyond the quadrupolar (Newtonian) order. Further, we employ the orbital binding energy and the time-eccentricity  $e_t$ , appearing in the PN-accurate generalized quasi-Keplerian parametrization for eccentric orbits [13], to characterize the inspiralling and precessing eccentric binaries. We explore the ability of various 2PN order circular templates to capture GW signals from compact binaries in inspiralling eccentric orbits by computing the fitting factors (FF), described in Ref. [14]. In the present study, the various 2PN order inspiral templates are provided by the adiabatic and complete adiabatic Taylor T1, the adiabatic Taylor T4 and the TaylorEt approximants [see Eqs. (15), (16), (17) and (18)].

The organization of the paper is as follows. In Sec. II, we briefly describe the phasing of GWs from compact binaries in inspiralling eccentric orbits, available in Ref. [10]. After that we provide certain PN-accurate formulae and relations that are necessary to construct our GW signals with the help of the lengthy PN-accurate expressions, available in Ref. [15]. Section II also contains formulae required to construct various types of circular templates. How and why we perform a number of FF computations are explained in Sec. III along with our results. Our conclusions are presented in Sec. IV.

## II. PHASING FORMULAE REQUIRED TO MODEL GW SIGNALS FROM ECCENTRIC BINARIES AND VARIOUS CIRCULAR TEMPLATES

This section provides brief descriptions and necessary formulae required to model GWs associated with non-spinning compact binaries inspiralling along eccentric and circular orbits. For the sake of simplicity, we only consider temporally evolving restricted  $h_{\times}(t)$ , having Newtonian accurate amplitude and PN-accurate phase evolution. In the case of compact binaries in inspiralling eccentric orbits, as noted earlier, we construct  $h_{\times}(t)$  by adapting the GW phasing formalism, available in Ref. [10]. This approach provides an efficient way of modeling the PN-accurate orbital dynamics of eccentric bina-

ries incorporating the three inherent time scales, namely, those associated with the radial motion (orbital period), advance of periastron, and radiation reaction, crucial to construct temporally evolving  $h_{\times}(t)$ . At present, the detailed PN-accurate expressions, describing the orbital dynamics of non-spinning compact binaries in 3PN-accurate eccentric orbits perturbed by the relative 2PN-accurate RR effects, computed with the help of Refs. [10, 13], are available in Ref. [15]. In the next subsection, we summarize what were detailed in Refs. [8, 10, 15] and obtain the restricted  $h_{\times}(t)$  associated with non-spinning compact binaries in precessing and inspiralling eccentric orbits in harmonic gauge. Due to the availability of the lengthy PN-accurate expressions in Ref. [15] that are useful to construct our fiducial GW signals, we only provide certain PN-accurate relations that are crucial to implement the the present version of the relevant  $h_{\times}(t)$  in the upcoming subsection. However, we do display all the formulae required to construct various types of circular templates that are employed in the present study.

### A. GW phasing for compact binaries in inspiralling PN-accurate eccentric orbits

The dominant quadrupolar contribution to the plus polarization, denoted by  $h_{\times}|_Q(t)$ , associated with a compact binary consisting of individual masses  $m_1$  and  $m_2$  at a radial distance  $R'$  [10] reads

$$\begin{aligned} h_{\times}(r(t), \phi(t), \dot{r}(t), \dot{\phi}(t))|_Q = & -\frac{2Gm\eta C}{c^4 R'} \left[ \left( \frac{Gm}{r(t)} + r(t)^2 \dot{\phi}(t)^2 \right. \right. \\ & \left. \left. - \dot{r}(t)^2 \right) \sin 2\phi(t) \right. \\ & \left. - 2\dot{r}(t)r(t)\dot{\phi}(t) \cos 2\phi(t) \right], \end{aligned} \quad (1)$$

where the symmetric mass ratio  $\eta = m_1 m_2 / m^2$  and  $m = m_1 + m_2$ , respectively, while  $C = \cos i$ ,  $i$  being the inclination of the orbital plane with respect to the plane of the sky. The orbital separation, phase and their time derivatives are denoted by  $r(t)$ ,  $\phi(t)$ ,  $\dot{r}(t) = dr(t)/dt$  and  $\dot{\phi}(t) = d\phi(t)/dt$ , respectively.

The phasing formalism, detailed in Ref. [10], provides an efficient way of implementing the temporal evolution for the dynamical variables,  $r(t)$ ,  $\phi(t)$ ,  $\dot{r}(t)$ ,  $\dot{\phi}(t)$ , appearing in Eq. (1). Following Ref. [10], we note that in the case of compact binaries in inspiralling eccentric orbits, however small may be the eccentricity, the time evolution of the dynamical variables explicitly depends on both the conservative and the reactive contribution to the orbital dynamics. Due to the existence of a Keplerian type parametric solution to the 3PN-accurate conservative orbital dynamics, detailed in Ref. [13], the conservative contributions to  $\{r(t), \phi(t), \dot{r}(t), \dot{\phi}(t)\}$  can be written as

$$r(t) = r(u(l), \mathcal{E}, \mathcal{J}), \quad (2a)$$

$$\dot{r}(t) = \dot{r}(u(l), \mathcal{E}, \mathcal{J}), \quad (2b)$$

$$\phi(t) = \lambda(l; \mathcal{E}, \mathcal{J}) + W(u(l), \mathcal{E}, \mathcal{J}), \quad (2c)$$

$$\dot{\phi}(t) = \dot{\phi}(u(l), \mathcal{E}, \mathcal{J}), \quad (2d)$$

where  $u$  and  $l$  are the eccentric and mean anomalies associated with the 3PN-accurate generalized quasi-Keplerian parametrization, respectively, while  $\mathcal{E}$  and  $\mathcal{J}$  stand for the orbital energy and angular momentum, respectively. The angular variable  $\phi$  is split into two parts to make sure that there exists a part that depends linearly on  $l$ . Recall that such a split allows one to explicate easily the effect of the periastron advance, while constructing the frequency spectrum associated with  $h_{\times}(t)$  relevant for compact binaries in PN-accurate eccentric orbits[see Ref. [16] for details]. The angular type variables  $\lambda$  and  $l$  can be expressed as

$$l \equiv n(t - t_0) + c_l = l(u; \mathcal{E}, \mathcal{J}, c_l), \quad (3a)$$

$$\lambda \equiv (1 + k)n(t - t_0) + c_{\lambda} = \lambda(t - t_0; \mathcal{E}, \mathcal{J}, c_{\lambda}), \quad (3b)$$

where the constants  $t_0$ ,  $c_l$  and  $c_{\lambda}$  refer to some initial instant and the values of  $l$  and  $\lambda$  at  $t = t_0$ . The symbols  $n$  and  $k$  represent the mean-motion and the measure of advance of the periastron in the time interval  $2\pi/n$ , respectively. It turns out that the PN-accurate expressions for  $n$  and  $k$  in terms of  $\mathcal{E}$  and  $\mathcal{J}$  are the only two gauge-invariant quantities present in the PN-accurate Keplerian-type parametric solution [13, 17]. If one ignores the reactive contributions to the orbital dynamics, the explicit temporal evolutions for the dynamical variables,  $r(t)$ ,  $\phi(t)$ ,  $\dot{r}(t)$ ,  $\dot{\phi}(t)$ , are obtained by solving the 3PN-accurate Kepler equation (KE) that provides the link between  $l$  and  $u$ . The 3PN-accurate KE can be symbolically expressed as

$$l = u - e_t \sin u + l_{2,3}(u, \mathcal{E}, \mathcal{J}), \quad (4)$$

where  $l_{2,3}(u, \mathcal{E}, \mathcal{J})$  stands for the 2PN and 3PN corrections to the usual Newtonian KE  $l = u - e_t \sin u$ . With the help of Eq. (4), we observe that the PN-accurate conservative dynamics, for example, specified by the 3PN-accurate relative acceleration  $\mathcal{A}^i$  in harmonic gauge[18], have *four* constants of integration, namely  $\mathcal{E}, \mathcal{J}, c_l$  and  $c_{\lambda}$ .

To describe the dynamics of compact binaries in inspiralling eccentric orbits, it is essential to include the reactive contributions to  $\mathcal{A}^i$  that first enters at the 2.5PN (absolute) order. However, it is imperative to invoke the energy and angular momentum balance argument to implement the higher order PN-accurate reactive evolution of an eccentric orbit. This is because the reactive contributions to  $\mathcal{A}^i$  are available only to the 1PN relative (or 3.5PN absolute) order [18]. Recall that the balance argument equates the orbital averaged higher order PN-accurate energy and angular momentum fluxes in GWs to the time derivatives of PN-accurate orbital energy and angular momentum, respectively. Invoking the balance argument and 2PN-accurate far-zone energy and angular

momentum fluxes, available in Refs. [19–21], it is possible to incorporate the 2PN-accurate secular RR effects on PN-accurate eccentric orbits in the following way[see Refs. [10, 15] for details]. To describe the inspiral dynamics of compact binaries, Ref. [10] employed an improved ‘method of variation of constants’ to include the RR effects onto the conservative orbital dynamics. The idea is to allow the dynamical variables, appearing in Eq. (1), have the same functional forms as given by Eqs. (2) and (3) even when the dynamics is not conservative, but reactive. However, one lets the associated constants of integration, namely  $\mathcal{E}, \mathcal{J}, c_l$  and  $c_{\lambda}$  to vary with time. The equations that govern the temporal evolutions of these quantities are given by Eqs. (35) in Ref. [10] and, as expected, depend on the reactive contributions to  $\mathcal{A}^i$ . Further, the temporal variations of these four constants of integration can be modeled to consist of a slow drift and fast oscillations, which symbolically reads

$$c_{\alpha}(l) = \bar{c}_{\alpha}(l) + \tilde{c}_{\alpha}(l), \quad (5)$$

where  $\alpha$  stands for one of the four quantities  $\mathcal{E}, \mathcal{J}, c_l$  and  $c_{\lambda}$ . In the above equation,  $\bar{c}_{\alpha}(l)$  denotes the slow drift, which accumulates over the RR time scale to induce large changes in  $c_{\alpha}(l)$ . The fast oscillations in  $c_{\alpha}(l)$  are denoted by  $\tilde{c}_{\alpha}(l)$ , and the explicit expressions for  $d\tilde{c}_{\alpha}/dt$  are only available to the relative 1PN order [15]. To the reactive PN order we are interested, it turns out that  $d\bar{c}_l/dt = d\bar{c}_{\lambda}/dt \equiv 0$ , while  $d\bar{\mathcal{E}}/dt$  and  $d\bar{\mathcal{J}}/dt$  are provided by the far-zone energy and angular momentum fluxes, respectively [10]. Further, it was demonstrated in Refs. [10, 15] that the rapidly oscillating parts have substantially smaller amplitudes. Therefore, for the present study, we ignore the RR induced  $\tilde{c}_{\alpha}(t)$  contributions to the orbital dynamics.

The strategy to obtain  $h_{\times}|_Q(t)$  associated with compact binaries moving in 3PN-accurate eccentric orbits that are perturbed by the relative 2PN-accurate RR effects is the following. With the help of the 3PN-accurate generalized quasi-Keplerian parametrization in harmonic coordinates, available in Ref. [13], and Refs. [10, 15], we compute the 3PN-accurate expressions for  $r, W, \dot{r}, \dot{\phi}$  in terms of  $\mathcal{E}, \mathcal{J}$  and  $u$ . This is supplemented by the 3PN-accurate expression for  $\lambda$  in terms of  $l, \mathcal{E}, \mathcal{J}$ . We employed a modified version of Mikkola’s method [22], detailed in Ref. [8], to solve accurately and efficiently the 3PN-accurate KE and obtain the temporal evolution for  $r(t), W(t), \dot{r}(t), \dot{\phi}(t)$  under the 3PN-accurate conservative orbital dynamics. Afterwards, we numerically solve the 2PN-accurate differential equations for  $\mathcal{E}$  and  $\mathcal{J}$  and impose the resulting reactive evolutions in  $\mathcal{E}$  and  $\mathcal{J}$  onto the earlier computed 3PN-accurate conservative orbital dynamics. The resulting  $r(t), \phi(t), \dot{r}(t), \dot{\phi}(t)$  leads to, via Eq. (1),  $h_{\times}|_Q(t)$  associated with non-spinning compact binaries inspiralling along 3PN-accurate eccentric orbits under the action of 2PN-accurate reactive dynamics.

Until now, we have employed the orbital energy and angular momentum to describe the eccentric inspiral.

However, a measure of the non-circularity is better described in terms of any of the eccentricity parameters, appearing in the PN-accurate Keplerian-type parametric solution [13], than in terms of  $\mathcal{J}$ . Therefore, from here onwards, we employ the orbital binding energy  $\mathcal{E}$  and the time eccentricity parameter  $e_t$ , associated with the PN-accurate KE, to specify our PN-accurate eccentric binaries. With the help of Ref. [15], it is fairly straightforward to obtain 3PN-accurate expressions for  $r, \dot{r}, \dot{\phi}, W, \lambda$  and 3PN-accurate KE in terms of  $\mathcal{E}$  and  $e_t$ . For the sake of brevity, we provide explicitly the above expressions

to 1PN order only. However, we do provide the 3PN-accurate relation connecting  $n$  to  $\mathcal{E}$  required to obtain the lengthy 2PN and 3PN corrections to  $r, \dot{r}, \dot{\phi}, W, \lambda$  and  $l(u)$  in terms of  $\mathcal{E}$  and  $e_t$  from Eqs. (23)-(27) in Ref. [15].

It should be noted that the dynamical variables enter  $h_{\times}|_Q(t)$  in certain combinations like  $\frac{Gm}{c^2 r}, \frac{r\dot{\phi}}{c}$  and  $\frac{\dot{r}}{c}$ . Therefore, we list below the following dimensionless dynamical variables required to describe the dynamical evolution of  $h_{\times}|_Q(t)$  in a partially symbolic manner.

$$\frac{Gm}{c^2 r}(\xi, e_t, u) = \frac{\xi}{\chi} \left\{ 1 + \xi \frac{1}{4\chi} [\chi(9 - 5\eta) + 6\eta - 16] + \xi^2(\dots) + \xi^3(\dots) \right\}^{-1} \quad (6a)$$

$$\frac{\dot{r}}{c}(\xi, e_t, u) = \frac{\xi^{1/2} e_t \sin u}{\chi} \left\{ 1 + \left[ \frac{3}{8} - \frac{9}{8}\eta \right] \xi + \xi^2(\dots) + \xi^3(\dots) \right\} \quad (6b)$$

$$\begin{aligned} \frac{r(\xi, e_t, u) \times \dot{\phi}(\xi, e_t, u)}{c} &= \frac{\xi^{1/2} \sqrt{1 - e_t^2}}{\chi} \times \left\{ 1 + \xi \frac{1}{4\chi} [\chi(9 - 5\eta) + 6\eta - 16] + \xi^2(\dots) + \xi^3(\dots) \right\} \times \left\{ 1 \right. \\ &\quad \left. + \xi \frac{1}{8(1 - e_t^2)} [-23 + 9\eta + e_t^2(15 - \eta) + \frac{1}{\chi} (32 - 8\eta + e_t^2(-32 + 8\eta))] + \xi^2(\dots) + \xi^3(\dots) \right\} \end{aligned} \quad (6c)$$

$$\phi(\xi, e_t, u, l) = \lambda(l, \xi, e_t, u) + W(\xi, e_t, u), \text{ where} \quad (6d)$$

$$\lambda(l, \xi, e_t, u) = \xi^{3/2} \frac{c^3}{Gm} \times \left\{ 1 + \xi \left[ \frac{1}{8}(-15 + \eta) + \frac{3}{(1 - e_t^2)} \right] + \xi^2(\dots) + \xi^3(\dots) \right\} (t - t_0) \quad (6e)$$

$$W(\xi, e_t, u)|_{1PN} = (v - u) + e_t \sin u + \xi \frac{3}{(1 - e_t^2)} \{ (v - u) + e_t \sin u \} + \xi^2(\dots) + \xi^3(\dots) \quad (6f)$$

where  $\xi = -2\mathcal{E}/\mu c^2$ ,  $\mu$  being the reduced mass of the binary:  $\mu = \eta m$  and  $\chi = (1 - e_t \cos u)$ . To evaluate  $W(\xi, e_t, u)$ , we employ the following expression for  $v - u$

$$v - u = 2 \tan^{-1} \left( \frac{\beta_\phi \sin u}{1 - \beta_\phi \cos u} \right), \quad (7)$$

where  $\beta_\phi = (1 - \sqrt{1 - e_\phi^2})/e_\phi$ . Using the PN accurate relation connecting  $e_\phi$  to  $e_t$ , extractable from Ref. [13], it is fairly straightforward to express  $\beta_\phi$  in terms of  $e_t$  and  $\xi$ . To 1PN order,  $\beta_\phi$  explicitly reads

$$\beta_\phi(\xi, e_t, \eta) = \frac{1 - \sqrt{1 - e_t^2}}{e_t} \left\{ 1 + \xi \frac{(4 - \eta)}{\sqrt{1 - e_t^2}} + \xi^2(\dots) + \xi^3(\dots) \right\} \quad (8)$$

The explicit expressions for the 2PN and 3PN contributions to  $Gm/c^2 r, \dot{r}/c, \lambda, W, r\dot{\phi}/c$  and  $\beta_\phi$ , symbolically noted as ‘ $+\xi^2(\dots) + \xi^3(\dots)$ ’ in their respective 1PN-

accurate expressions, are obtainable in a straightforward manner using Eqs. (23)-(26) in Ref. [15] and the following 3PN-accurate expression connecting  $n$  to  $\xi$  and  $e_t$  [13]

$$n = \xi^{3/2} \frac{c^3}{Gm} \left\{ 1 - \xi \frac{1}{8} [15 - \eta] + \xi^2 \frac{1}{128} \left[ (555 + 30\eta + 11\eta^2) - \frac{1}{\sqrt{1 - e_t^2}} (960 - 384\eta) \right] \right\}$$

$$+ \xi^3 \frac{1}{3072(1-e_t^2)^{3/2}} \left[ 16 \left( -2340 + \{10244 - 123\pi^2\}\eta - 792\eta^2 - 36 e_t^2 \{255 - 159\eta + 34\eta^2\} \right) + \right. \\ \left. (1 - e_t^2)^{3/2} \left( 45(-653 - 111\eta - 7\eta^2 + 3\eta^3) \right) \right] \Bigg\} \quad (9)$$

The explicit conservative temporal evolution for the above listed orbital variables are obtained by solving the

3PN-accurate KE connecting  $u$  to  $l$ . The right hand side of the PN-accurate KE reads

$$l(\xi, u, e_t) = u - e_t \sin u + \xi^2 \left\{ \frac{(\frac{15}{2} - 3\eta)(v - u)}{\sqrt{1 - e_t^2}} + \frac{e_t(15 - \eta)\eta \sin(u)}{8\chi} \right\} + \xi^3 (..) \quad (10)$$

where the  $v - u$  term appearing at the 2PN order on the right hand side of Eq. (10) is evaluated using 1PN-accurate expression for  $\beta_\phi$ . As noted earlier, for an accurate and efficient determination of  $u(l)$ , we employed a modified version of Mikkola's method for solving the classical KE [22](see Ref. [8] for its implementation at the 2PN order). With the help of PN-accurate  $u(l)$ , it is fairly easy to obtain  $h_\times|_Q(t)$  associated with compact binaries evolving under 3PN-accurate conservative orbital dynamics.

Let us now impose the effects of 2PN-accurate RR onto the above detailed conservative orbital dynamics. Due to the neglect of the small amplitude and fast oscillatory contributions to  $\mathcal{E}$ ,  $\mathcal{J}$ ,  $c_l$  and  $c_\lambda$ , the reactive orbital evolution is entirely given by 2PN-accurate orbital averaged expressions for the energy and angular momentum fluxes, and these PN-accurate expressions in harmonic

gauge can be extracted from Refs. [19–21]. However, in this study, the PN-accurate eccentric orbits are specified in terms of  $\xi$  and  $e_t$ , and hence require the 2PN-accurate differential equations for  $\xi$  and  $e_t$ , written in terms of  $\xi$  and  $e_t$ . Due to the definition of  $\xi$ , the differential equation governing the reactive evolution of  $\xi$  follows directly from the 2PN-accurate far-zone energy flux. The differential equation describing the secular 2PN-accurate reactive evolution of  $e_t$ , requires i) the 2PN accurate expression for  $e_t^2$  in terms of  $\mathcal{E}$  and  $\mathcal{J}$  in harmonic gauge, available in Ref. [13], ii) the 2PN-accurate expressions for the orbital averaged far-zone energy and angular momentum fluxes and finally iii) the energy and angular momentum balance argument. The resulting 2PN-accurate expressions for  $d\xi/dt$  and  $de_t/dt$ , describing the secular evolutions of  $\xi$  and  $e_t$ , is given by

$$\frac{d\xi}{dt} = 2 \frac{\xi^5 \eta^2}{15} \frac{c^3}{Gm} \left\{ \dot{\xi}^N + \dot{\xi}^{1PN} + \dot{\xi}^{1.5PN} + \dot{\xi}^{2PN} \right\}, \quad (11a)$$

$$\frac{de_t}{dt} = -\frac{\xi^4 e_t \eta}{15} \frac{c^3}{Gm} \left\{ \dot{e}_t^N + \dot{e}_t^{1PN} + \dot{e}_t^{1.5PN} + \dot{e}_t^{2PN} \right\}, \text{ where} \quad (11b)$$

$$\dot{\xi}^N = \frac{1}{(1 - e_t^2)^{7/2}} \{96 + 292e_t^2 + 37e_t^4\} \quad (11c)$$

$$\dot{\xi}^{1PN} = \frac{\xi}{56(1 - e_t^2)^{9/2}} \{208 - 13440\eta + 8[22340 - 19607\eta]e_t^2 + 42[5966 - 3459\eta]e_t^4 + [19487 - 8806\eta]e_t^6\} \quad (11d)$$

$$\dot{\xi}^{1.5PN} = \frac{\xi^{3/2}\pi}{96} \{36864 + 448320e_t^2 + 2061840e_t^4 + 6204647e_t^6\}, \quad (11e)$$

$$\dot{\xi}^{2PN} = \frac{\xi^2}{6048(\sqrt{1 - e_t^2})^{11}} \{32 [253937 - 162585\eta + 45360\eta^2] + 16 [2007326 - 6275466\eta + 3509541\eta^2] e_t^2 \\ + 12 [22179502 - 35103402\eta + 13897611\eta^2] e_t^4 + 18 [12638659 - 12297567\eta + 3878616\eta^2] e_t^6 \\ + 9 [1374197 - 916728\eta + 254856\eta^2] e_t^8 - 9072 [96 - 1060e_t^2 - 1863e_t^4 - 148e_t^6] \sqrt{1 - e_t^2} (5 - 2\eta)\}, \quad (11f)$$



$$\dot{e}_t^N = \frac{(121e_t^2 + 304)}{(\sqrt{1-e_t^2})^5}, \quad (11g)$$

$$\dot{e}_t^{1PN} = \frac{\xi}{56(\sqrt{1-e_t^2})^7} \left[ \{75667e_t^4 + 344784e_t^2 - 980(34e_t^4 + 225e_t^2 + 72)\eta - 28536\} \right], \quad (11h)$$

$$\dot{e}_t^{1.5PN} = \frac{\xi^{3/2}\pi}{96} \left[ 189120 + 1042992e_t^2 + 3061465e_t^4 \right], \quad (11i)$$

$$\begin{aligned} \dot{e}_t^{2PN} = & \frac{\xi^2}{2016(\sqrt{1-e_t^2})^9} \left[ (17914878 - 12062097\eta + 3288852\eta^2)e_t^6 \right. \\ & + (128983907 - 139206105\eta + 45633420\eta^2)e_t^4 + (46339524\eta^2 - 94111416\eta + 28071312)e_t^2 \\ & \left. + 7116856 - 6772968\eta + 3566304\eta^2 + 3024(511e_t^4 + 2809e_t^2 + 80)(5-2\eta)\sqrt{1-e_t^2} \right]. \end{aligned} \quad (11j)$$

The contributions entering at the relative 1.5PN order are due to the dominant order GW tails that are usually expressed in terms of certain infinite sums involving the Bessel functions  $J_p(pe_t)$  and its derivative  $J'_p(pe_t)$  [19, 20]. In the above equations, we have expanded those infinite sums to  $\mathcal{O}(e_t^4)$ . This is justified as we are only interested in eccentric binaries having initial  $e_t \leq 0.2$  in the present study. Let us remind the reader that it is due to the neglect of the *tilde* contributions to  $\mathcal{E}, e_t, c_l$  and  $c_\lambda$  that the reactive evolution is fully prescribed by the above differential equations for  $\xi(t)$  and  $e_t$ . And, the above two equations represent the secular variations in  $\xi$  and  $e_t$ , namely  $\bar{\xi}(t)$  and  $\bar{e}_t(t)$ , due to the emission of GWs.

We are now in a position to implement numerically  $h_\times|_Q(t)$  emanating from non-spinning compact binaries inspiralling along 3PN-accurate eccentric orbits under the action of 2PN-accurate reactive dynamics. It is obvious that we need to specify the initial and final val-

ues for  $\xi$  so that the dominant GW spectral component of  $h_\times|_Q(t)$  evolves in the frequency window 40Hz -  $(6^{3/2}\pi Gm/c^3)^{-1}$  Hz, relevant for the initial LIGO. We compute the bounding values for  $\xi$  with the help of Ref. [16] that demonstrated the fact that the dominant GW spectral component of a mildly eccentric compact binary, having PN accurate orbital motion, appears at  $\frac{1}{\pi} < \frac{d\phi}{dt} > \equiv \frac{n(1+k)}{\pi}$ , where  $< \frac{d\phi}{dt} >$  stands for the PN-accurate orbital average of  $d\phi/dt$ . The PN-accurate expression for  $< \frac{d\phi}{dt} >$  can be computed using the procedure, detailed in Ref. [23], involving the Laplace second integrals for the Legendre polynomials[see Eqs. (4.16)-(4.19) in Ref. [23]]. For the present paper, we use the following 3PN-accurate expression for the orbital averaged orbital angular velocity  $< \frac{d\phi}{dt} >$  to obtain the bounding values for  $\xi$  for a compact binary specified by certain  $m, \eta$  and  $e_t$  values:

$$\begin{aligned} \left\langle \frac{d\phi}{dt} \right\rangle & \equiv n(1+k) \\ & = \xi^{\frac{3}{2}} \frac{c^3}{Gm} \left\{ 1 + \xi \left[ \frac{\eta}{8} + \frac{3}{1-e_t^2} - \frac{15}{8} \right] + \frac{\xi^2}{128(1-e_t^2)^2} \left[ (1851 - 786\eta + 11\eta^2) - 2e_t^2(-861 + 486\eta + 11\eta^2) \right. \right. \\ & \quad + e_t^4(555 + 30\eta + 11\eta^2) + 192(1-e_t^2)^{3/2}(-5 + 2\eta) \left. \right] + \frac{\xi^3}{3072(1-e_t^2)^3} \left[ 3(76965 + (-167089 + 3936\pi^2)\eta \right. \\ & \quad + 5439\eta^2 + 45\eta^3) + 3e_t^2(228249 + (-222781 + 984\pi^2)\eta + 40491\eta^2 - 135\eta^3) + 9e_t^4(25301 - 17201\eta + 3471\eta^2 \\ & \quad + 45\eta^3) - 45e_t^6(-653 - 111\eta - 7\eta^2 + 3\eta^3) + \sqrt{1-e_t^2}(16(-6660 - 41(-292 + 3\pi^2)\eta - 792\eta^2 \\ & \quad \left. \left. + e_t^2(6120 + (-9704 + 123\pi^2)\eta - 432\eta^2) + 36e_t^4(255 - 159\eta + 34\eta^2))) \right] \right\} \end{aligned} \quad (12)$$

With these inputs, it is fairly straightforward to construct

$h_\times|_Q(t)$  for inspiralling compact binaries, having some

tiny orbital eccentricity, emitting GWs in the initial LIGO frequency window.

Finally, let us explain why we employed  $\xi$ , along with  $e_t$ , to represent the PN-accurate eccentric orbit, which guided us to use  $\xi$  as our PN expansion parameter. In the literature, the GW phasing for eccentric binaries are performed using either  $(\frac{Gm\eta}{c^3})^{(2/3)}$  [10, 15] or  $(\frac{Gm\omega}{c^3})^{(2/3)}$  [24, 25], where  $\omega$  stands for the above listed 3PN-accurate  $\langle \frac{d\phi}{dt} \rangle$ , as the PN expansion parameters, along with  $e_t$ . The choice of  $n = 2\pi/T_r$ , where the radial period  $T_r$  being the time of return to the periastron, as a PN expansion parameter may be visually problematic. This is because it is rather difficult to pinpoint the periastron position for circular binaries, making it difficult to imagine the meaning of  $T_r$  in the case of circular inspiral. We speculate that this may be the one of the reasons for Ref. [24] to introduce  $\omega \equiv \langle \frac{d\phi}{dt} \rangle = n(1+k)$  as their PN expansion parameter. However, it is not clear why one should employ the orbital averaged angular velocity to perform GW phasing for eccentric binaries. The reason stated in Ref. [24] for introducing  $\langle \frac{d\phi}{dt} \rangle$  as the PN-expansion parameter is that it generalizes the  $\omega = d\phi/dt$  parameter used in the construction of the usual PN-accurate inspiral templates, available in Ref. [4]. In other words, the PN accurate expression for  $d\phi/dt$ , given in terms of  $\xi, e_t, u$ , when re-expressed in terms  $\omega \equiv \langle \frac{d\phi}{dt} \rangle, e_t, u$  using Eq. (12) will lead to  $d\phi/dt = \omega$  in the circular limit [check Eqs. (A.10)-(A.14) in Ref. [25] for the actual demonstration of the above statement]. It is important to realize that the use of  $d\phi/dt = \omega$  as the PN expansion parameter for the circular inspiral is usually justified by the argument that it defines the instantaneous orbital angular frequency. In the case of the heavily employed restricted PN-accurate inspiral templates [4], the instantaneous GW frequency  $f_{\text{GW}}$  is related to the instantaneous orbital angular frequency by  $f_{\text{GW}} \equiv \omega/\pi$ . However, in the case of GW phasing for eccentric binaries, neither  $n$  nor  $\omega \equiv \langle \frac{d\phi}{dt} \rangle$  are sufficient to define the instantaneous orbital angular frequency. Further, the associated GW spectrum can not be expressed solely in terms of  $n$  or  $\langle \frac{d\phi}{dt} \rangle$  [8]. These considerations prompted us to employ neither  $n$  nor  $\omega \equiv \langle \frac{d\phi}{dt} \rangle$  as our PN expansion parameter for performing the GW phasing for eccentric binaries. We would like to stress that, while considering the PN-accurate conservative orbital dynamics, our PN expansion parameter requires no orbital averaging or any prior knowledge about the turning points of the associated eccentric orbit. Further,  $\xi$  provides a measure of the instantaneous orbital energy of an eccentric orbit. In the case of circular inspiral, it is also straightforward to identify  $\xi$  as a measure for the instantaneous orbital energy. Interestingly, for Newtonian circular orbits, our PN expansion parameter  $\xi$  is indeed a measure of  $\frac{v^2}{c^2}$  like  $(\frac{Gm\eta}{c^3})^{2/3}$  and  $(\frac{Gm\omega}{c^3})^{2/3}$  variables available in the literature.

It was argued in Ref. [10] that the GW phasing for eccentric binaries that employ  $n$  as the PN expansion

parameter is not going to be accurate near the last stable orbit (LSO). This is one of the reasons for terminating the eccentric orbital evolution around  $j^2 \sim 48$  in Refs. [10, 15], where  $j = c\mathcal{J}/Gm\mu$ . Recall that for a test particle around a Schwarzschild black hole, the last stable circular orbit is also given by  $j^2 = 12$  [17]. A recent comparison between PN and Numerical Relativity (NR) based GW phase evolutions for equal-mass eccentric binaries, reported in Ref. [25], also supported the above argument. However, Ref. [25] demonstrated that the PN-accurate GW phasing for eccentric binaries, having 3PN-accurate conservative and 2PN accurate reactive dynamics, that employ  $\omega \equiv \langle \frac{d\phi}{dt} \rangle$  as the PN expansion parameter are fairly accurate even near the LSO. This observation can be linked to the fact that the GW phasing for eccentric binaries in terms of  $\omega \equiv \langle \frac{d\phi}{dt} \rangle$  and  $e_t$ , in the limit  $e_t \rightarrow 0$  provides the 2PN-accurate TaylorT4 approximant. And, Refs. [12, 26] recently demonstrated that the GW phase evolution under this TaylorT4 approximant is fairly close to its NR counterpart for equal mass binary black holes having around 10-15 orbital cycles close to their LSOs. We would like to point out that in the limit  $e_t \rightarrow 0$ , our present prescription for doing GW phasing for eccentric binaries leads to the TaylorEt approximant that employ the 3PN accurate expression for  $d\phi/dt$  and the 2PN accurate expression for  $d\xi/dt$  [11]. With the help of Fig. 4 in Ref. [26], we can state that the accumulated GW phase difference between the above approximant and NR, during the late inspiral stage of an equal-mass binary, is comparable to what is provided the TaylorT4 approximant at 2.5PN order. The above phase difference turned out to be substantially smaller than a similar accumulated GW phase difference originating from a 2PN approximant that employs  $(\frac{Gm\eta}{c^3})^{2/3}$  as the PN expansion parameter [11]. Therefore, it is reasonable to expect that during the late inspiral stage, our present prescription for doing eccentric GW phasing could be closer to NR than what is presented in Refs. [10, 15]. We are initiating an effort to make such a comparison with the help of yet-to-be available fully 3PN-accurate RR effects for the eccentric inspiral, similar to what is reported in Ref. [26].

In what follows, we briefly describe how we construct various PN-accurate circular inspiral templates that incorporate RR effects to the relative 2PN accuracy.

## B. Various PN-accurate circular inspiral templates that incorporate RR effects at the relative 2PN order

In this subsection, we briefly describe how to construct the earlier mentioned PN-accurate templates relevant for the circular inspiral. The crucial PN-accurate quantities that are required to construct these circular inspiral templates are the 3PN-accurate orbital binding energy  $\mathcal{E}(x)$  [18, 27] and the 2PN-accurate GW luminosity  $\mathcal{L}(x)$  [28], both of which are usually expressed as PN series in the

gauge invariant quantity  $x \equiv (G m \omega / c^3)^{2/3}$ , where  $\omega$  is the instantaneous orbital angular frequency of the asso-

ciated circular binary. The explicit expressions for  $\mathcal{E}(x)$  and  $\mathcal{L}(x)$  relevant for the present study are

---


$$\mathcal{E}(x) = -\frac{\eta m c^2}{2} x \left\{ 1 - \frac{1}{12} [9 + \eta] x - \left[ \frac{27}{8} - \frac{19}{8} \eta + \frac{1}{24} \eta^2 \right] x^2 - \left[ \frac{675}{64} + \left( \frac{205}{96} \pi^2 - \frac{34445}{576} \right) \eta + \frac{155}{96} \eta^2 + \frac{35}{5184} \eta^3 \right] x^3 \right\}, \quad (13a)$$

$$\mathcal{L}(x) = \frac{32 \eta^2 c^5}{5 G} x^5 \left\{ 1 - \left[ \frac{1247}{336} + \frac{35}{12} \eta \right] x + 4 \pi x^{3/2} - \left[ \frac{44711}{9072} - \frac{9271}{504} \eta - \frac{65}{18} \eta^2 \right] x^2 \right\}, \quad (13b)$$


---

The time-domain  $x$ -based circular templates are also constructed under the restricted PN-accurate prescription and this leads to

$$h_{\times} = -\frac{4 G m \eta C}{c^2 R'} x(t) \sin 2 \phi(t), \quad (14)$$

Following Refs. [4, 9], one can construct different template families that provide different prescriptions for the evolution of  $x(t)$  and  $\phi(t)$  appearing in the above equation. The 2PN order adiabatic TaylorT1 approximant of Ref. [4] is given by

$$\frac{d\phi(t)}{dt} = \omega(t) \equiv \frac{c^3}{G m} x^{3/2}, \quad (15a)$$

$$\frac{dx(t)}{dt} = -\frac{\mathcal{L}(x)}{(d\mathcal{E}_{2PN}/dx)}, \quad (15b)$$

where  $\mathcal{E}_{2PN}$  stands for the 2PN-accurate orbital binding energy, obtainable by dropping  $x^3$  terms in Eq. (13a) for

$\mathcal{E}(x)$ . It should be noted that in this approximant, available in LAL, one truncates the PN-accurate expressions for  $\mathcal{E}(x)$  and  $\mathcal{L}(x)$  at the same relative PN order. We can also create the complete adiabatic TaylorT1 approximant in the following way [9]

$$\frac{d\phi(t)}{dt} = \omega(t) \equiv \frac{c^3}{G m} x^{3/2}, \quad (16a)$$

$$\frac{dx(t)}{dt} = -\frac{\mathcal{L}(x)}{(d\mathcal{E}/dx)}, \quad (16b)$$

where  $\mathcal{E}(x)$  is indeed 3PN-accurate and is given by Eq. (13a).

The TaylorT4 approximant, introduced in Ref. [12], is obtained by Taylor expanding in  $x$  the right-hand-side of either Eq. (15b) or Eq. (16b) to the 2PN order in  $x$ . The 2PN-accurate TaylorT4 is defined by

---


$$\frac{d\phi(t)}{dt} = \omega(t) \equiv \frac{c^3}{G m} x^{3/2}, \quad (17a)$$

$$\frac{dx(t)}{dt} = \frac{c^3}{G m} \frac{64 \eta}{5} x^5 \left\{ 1 - \left( \frac{743}{336} + \frac{11}{4} \eta \right) x + 4 \pi x^{3/2} + \left( \frac{34103}{18144} + \frac{13661}{2016} \eta + \frac{59}{18} \eta^2 \right) x^2 \right\}. \quad (17b)$$


---

While searching for inspiral GWs, the LSC employs (or has employed even in the recent past) the Fourier domain 2PN-accurate TaylorF2 approximants [5]. This approximant can be constructed analytically from the above TaylorT4 approximant using the stationary phase approximation [29] making it computationally cheaper than the time-domain TaylorT4 approximant. However, the focus of the present study is not the computational costs associated with the implementation of various template

families, therefore, we employed the 2PN-accurate time-domain TaylorT4 approximant rather than its Fourier domain counterpart. We observe that among the three approximants, the LSC Algorithm Library (LAL)[30] strictly provides only one of them, namely, the adiabatic TaylorT1 approximant at the 2PN order.

Finally, we construct the 2PN version of the TaylorEt using Ref. [11] as



$$h(t) = -\frac{4 G m \eta C}{c^2 R'} \xi(t) \sin 2 \phi(t), \quad (18a)$$

$$\begin{aligned} \frac{d\phi(t)}{dt} \equiv \omega(t) = & \frac{c^3}{G m} \xi^{3/2} \left\{ 1 + \frac{1}{8} (9 + \eta) \xi + \left[ \frac{891}{128} - \frac{201}{64} \eta + \frac{11}{128} \eta^2 \right] \xi^2 \right. \\ & \left. + \left[ \frac{41445}{1024} - \left( \frac{309715}{3072} - \frac{205}{64} \pi^2 \right) \eta + \frac{1215}{1024} \eta^2 + \frac{45}{1024} \eta^3 \right] \xi^3 \right\}, \end{aligned} \quad (18b)$$

$$\frac{d\xi(t)}{dt} = \frac{c^3}{G m} \frac{64}{5} \eta \xi^5 \left\{ 1 + \left( \frac{13}{336} - \frac{5}{2} \eta \right) \xi + 4 \pi \xi^{3/2} + \left( \frac{117857}{18144} - \frac{12017}{2016} \eta + \frac{5}{2} \eta^2 \right) \xi^2 \right\}, \quad (18c)$$

The above approximant obviously provides the circular limit of GW phasing for eccentric inspiral, detailed in the previous subsection, and hence employ  $\xi$  as the PN expansion parameter. A number of features of this approximant are worth mentioning. The TaylorEt approximant is specified by two separate PN-accurate differential equations and in contrast, the various  $x$ -based approximants are governed by just one PN-accurate differential equation. In a given GW frequency band, the limits of the integration for various  $x$ -based approximants, irrespective of whether one is interested in the Newtonian or 3.5PN order approximant, are the same and are independent of the symmetric mass ratio  $\eta$ . However, the limits of the integration for the TaylorEt approximant do depend on the underlying 3PN-accurate conservative dynamics and therefore depend on  $\eta$ .

The plots of  $H_{\times}(t)$  representing  $h_{\times}|_Q(t)$  scaled by  $G m \eta C / c^2 R'$  evolving under various prescriptions detailed in this section are displayed in Fig. 1. These plots, displaying the evolving  $H_{\times}(t)$  in the initial-LIGO frequency window, represent the canonical neutron star-black hole binary. The plots are for i) an eccentric binary inspiralling with an initial  $e_t = 10^{-3}$ , ii) the TaylorEt approximant, iii) the adiabatic TaylorT1 approximant and iv) the TaylorT4 approximant. The similar duration for the eccentric and the circular TaylorEt  $H_{\times}(t)$  should be noted.

Let us now move on to explore the ability of various circular templates to capture GWs from inspiralling compact binaries having tiny orbital eccentricities.

### III. PERFORMANCES OF VARIOUS CIRCULAR TEMPLATES AGAINST GW SIGNALS FROM COMPACT BINARIES IN INSPIRALLING ECCENTRIC ORBITS

In this section, we explore how effectual and faithful are the various 2PN order circular templates, introduced in the previous section, with respect to GW signals from compact binaries in inspiralling eccentric orbits that should be interesting to the initial-LIGO data analysts. This is achieved by computing the fully maximized overlaps involving the eccentric  $h_{\times}(t)$ , treated to be the

fiducial inspiral GW signal, and the *four* types of circular inspiral templates, given by Eqs. (15), (16), (17) and (18). We extensively employ Ref. [14] to compute the fully maximized overlaps with the help of their minimax overlap. In our numerical experiments, the maximization over the time-lags are straightforward as we invoke the fast-Fourier-transform routine of the Numerical Recipes [31] to compute the Fourier-domain versions of our time-domain GW signals and templates. Further, the maximization over  $m$  and  $\eta$ , characterizing the various circular templates are performed using the *amoeba* routine[31]. In the present context, a given circular template family is considered to be effectual and faithful if some members of the family can provide fully maximized overlaps, hereon the fitting factors (FFs), that are closer to unity and have smaller biases in estimating the parameters representing our fiducial GW signal. In other words, the values of  $m$  and  $\eta$  characterizing the circular template having the largest FF provide a measure of the faithfulness of that particular template family. It turns out that the drop in event rate is proportional to  $(1 - \text{FF}^3)$  [32] and therefore, it is indeed desirable to have circular template families having FF values that are  $\geq 0.97$  with respect to fiducial GW signals from compact binaries having tiny orbital eccentricities. This is mainly because the expected astrophysical GW sources will have tiny, but non-zero, orbital eccentricities.

In Table I, we show the FFs involving our fiducial eccentric GW signals and the 2PN order TaylorT4 circular templates, relevant for the initial LIGO. We restrict our attention to the usual canonical binaries representing neutron star-neutron star, black hole-neutron star and black hole-black hole binaries. In our FF computations, we evolve both our fiducial GW signals and circular templates in the frequency range 40 Hz to  $(6^{3/2} \pi G m / c^3)^{-1} \text{Hz}$ . The numbers clearly indicate that the 2PN TaylorT4 circular templates are neither effectual nor faithful in extracting our fiducial GW signals from inspiralling binaries, having low orbital eccentricities like  $e_t \sim 0.001$ . The numbers associated with the  $e_t = 10^{-3}$  case are representative of what to expect for still lower values for the initial  $e_t$ . We justify the above statement by repeating the FF computation employing the circular TaylorEt approximant to model the fiducial

GW signal. And, the resulting numbers are listed in the first row of Table I.

Next in Table II, we show the results of our FF computation involving the adiabatic and complete adiabatic TaylorT1 circular templates that require 2PN accurate RR effects. The complete adiabatic TaylorT1 templates are invoked so that we can include the effects of 3PN-accurate conservative orbital dynamics into the usual  $x$ -based circular templates that require the 2PN-accurate reactive dynamics, given by Eqs. (13). The circular TaylorEt approximant is again invoked to model our fiducial GW signal mainly to point out that the FFs are not improved for binaries having initial  $e_t < 0.001$ .

The performances of the TaylorEt circular templates against our fiducial GW signals from eccentric binaries are compared in Table III. The numbers, not surprisingly, demonstrate that the circular inspiral templates based on the TaylorEt approximant is both effectual and faithful in capturing GWs from compact binaries having tiny orbital eccentricities. The listed biases in the total masses of the canonical binaries are consistent with the fact that both eccentricity and higher values for the total mass are capable of decreasing the number of GW cycles in a given GW frequency window.

The numbers displayed in Tables I and II clearly indicate that GW signals from inspiralling compact binaries having tiny orbital eccentricities, constructed by adapting the phasing formalism, detailed in Ref. [10, 15] and summarized in Sec. II, can not be captured by the usual  $x$ -based adiabatic and complete adiabatic TaylorT1 and adiabatic TaylorT4 circular templates that incorporate the 2PN-accurate reactive dynamics. This is should be of definite concern for the GW community because the expected GWs from astrophysical compact binaries will have tiny orbital eccentricities and the GW data analysts belonging to the LSC employed, even in the recent past, the traditional  $x$ -based 2PN order circular inspiral templates to search for GWs from non-spinning compact binaries [5]. The numbers displayed in Tables I and II evince that the dominant reason for the above unexpected conclusion is the inability of the  $x$ -based circular inspiral templates, based on the two TaylorT1 and T4 approximants, to capture GW signals modeled after the TaylorEt approximant, in an effectual and faithful manner.

From a purely mathematical point of view, it may be argued that the circular TaylorEt and  $x$ -based approximants should be identical as they differ only in the use of the PN-expansion parameter. This implies that the observed differences in GW phase evolutions under various PN approximants may be attributed to the uncontrolled higher order terms. However, the present analysis and the one detailed in Ref. [33] indicate that for the data analysis considerations the inspiral templates belonging to the TaylorEt and the  $x$ -based approximants should be treated to be different. From a physical point of view, these approximants are also different due to the following reasons. It should be noted that due to the

use of the standard energy balance argument, various circular inspiral templates model GWs from compact binaries evolving along a sequence of circular orbits under the action of gravitational radiation reaction. For the  $x$ -based templates, the above circular orbits can be treated to be Newtonian-accurate due to the use of Eq. (15a) for  $d\phi/dt$ . However, the TaylorEt approximant requires the 3PN-accurate expression for  $d\phi/dt$  and therefore the sequence circular orbits can be considered to be 3PN-accurate. The differences in the above mentioned circular orbits imply that the TaylorEt approximant is specified by two separate PN-accurate differential equations, while the TaylorT1 and TaylorT4 approximants are governed by just one PN-accurate differential equation. Further and as noted earlier, for a given GW frequency window, the limits of the integration for the  $x$ -based approximants, irrespective of whether one is interested in Newtonian or 3.5PN accurate templates, are the same and are independent of  $\eta$ . However, the limits of the integration for the TaylorEt approximant in the present study crucially depend on the underlying 3PN-accurate conservative dynamics and do depend on  $\eta$ .

It may be argued that if one constructs eccentric GW signals using the generalized  $x$  parameter, introduced in an ad-hoc manner in Refs. [24, 25], and  $e_t$ , the 2PN order TaylorT4 approximant (and hence LSC's 2PN-accurate TaylorF2 approximant) will have no difficulty in capturing such eccentric GW signals. This is because the TaylorT4 approximant indeed provides the circular limit of GW phasing for eccentric binaries that employ the generalized  $x$  parameter and  $e_t$ . Let us (again) recall that the use of  $\omega \equiv d\phi/dt$  as a PN expansion parameter for the circular inspiral is justified due to the fact that it provides the instantaneous orbital angular frequency. Further, the emitted instantaneous GW angular frequency is related to its orbital counterpart by a factor of two in the case the restricted PN-accurate circular templates. However, as noted in the previous section and clearly visible in Eqs. (A10)-(A14) in Ref. [25], the PN expansion parameter  $\omega \equiv < d\phi/dt >$  present in the generalized  $x$  parameter *will not* provide the instantaneous orbital angular frequency in the case of compact binaries in inspiralling eccentric orbits. Further, the GW spectrum associated with compact binaries in PN-accurate eccentric orbits *is not* expressible as integer multiples of  $< d\phi/dt > = n(1+k)$  [8]. Therefore, it is not clear why one should employ  $\omega \equiv < d\phi/dt >$  as the PN expansion parameter to perform GW phasing for eccentric binaries, when there exists a more primary and gauge-invariant variable like  $\xi$  that is related to the binary's instantaneous orbital energy.

The practitioners and proponents of the  $x$ -based inspiral  $h_{\times,+}(t)$ , both circular and eccentric, may point out that the PN-accurate GW phasing for eccentric binaries in terms of the generalized  $x$  parameter and  $e_t$  are closer to what is provided by NR, as reported in Ref. [25]. In our opinion, this is most likely due to the ability of the circular 2PN-accurate TaylorT4 approximant to

track fairly closely the GW phase evolution, originating from NR, associated with the equal-mass binary black hole inspirals that last several orbits near their respective last stable orbits[12, 26]. An inspection of Fig. 4 in Ref. [26] reveals that at the 2PN reactive order the accumulated GW differences between TaylorEt-TaylorT1 and TaylorEt-TaylorT4 are  $\sim 4.4$  radians and  $\sim 2.6$  radians, respectively. These differences in the accumulated GW phase may be attributed to the uncontrolled higher order terms present in the various Taylor approximants and are partially responsible for our FF results. The statement about the partial responsibility is due to our observation that both the TaylorT1 and T4 approximants are fairly effectual in capturing GWs from equal mass circular compact binaries, based on the TaylorEt approximant and having  $m \geq 30 M_\odot$ . However, these  $x$ -based approximants are not effectual (and faithful) in the case of low mass binaries. We note that similar results prevail even when the RR order is increased to the 3.5PN relative order while dealing with equal-mass circular inspirals[33]. This is despite the observation that the GW phase evolution under the circular TaylorEt approximant at 3.5PN order is fairly close to NR (and hence to the TaylorT4 approximant at 3.5PN order) in comparison with what is provided by the TaylorEt approximant at the 2PN reactive order [26].

The Fig. 4 in Ref. [26] indicates that the PN-accurate GW phase evolutions prescribed by the circular TaylorEt and TaylorT4 approximants at 2.5PN reactive order can not be substantially different from each other. Therefore, it is natural to expect that these two approximants will be effectual and faithful to each other for data analysis considerations. The entries listed in Table IV support somewhat different conclusions, similar to what is detailed in Ref. [33]. In other words, for low  $m$  compact binaries, the TaylorT4 approximant is not effectual and in the case of high  $m$  binaries, the  $x$ -based approximant is effectual at the expense of inviting some what large biases in  $\eta$ .

The earlier discussions that supported the use of  $\xi$  as an appropriate PN expansion parameter for doing GW phasing for eccentric binaries and the monotonic convergence to the NR based GW phase evolution, exhibited by its circular counterpart, suggest that the TaylorEt approximant at 3.5PN order is a promising candidate to search for inspiral GWs from astrophysical compact binaries that are surely going to have tiny orbital eccentricities. Further, the Fig.4 in Ref. [26] reveals that the accumulated phase disagreement between the 3.5PN order TaylorEt approximant and 2PN order TaylorT4 approximant is  $\sim 1.00$  radians while considering an equal-mass binary inspiral that last around nine orbits during its late inspiral stage. Therefore, we probed how effectual and faithful are these two distinct approximants and the results are listed in Table V. We observe that FFs that are greater than 0.97 are only possible for binaries that have  $m > 35 M_\odot$  and for other stellar mass binaries, the 2PN order TaylorT4 templates are fairly inef-

fectual. It is worthwhile to note that this experiment is also prompted by the observation that the LSC employed 2PN-accurate TaylorF2 templates that are identical to the 2PN-accurate TaylorT4 approximant for data analysis considerations [5].

It is plausible that the inability of the 2PN-accurate TaylorT4 approximant to capture inspiral GWs modeled after the TaylorEt approximant or its eccentric extension can have astrophysical implications. Recently, the LSC reported that it is rather impossible to have a compact binary progenitor for the gamma-ray-burst GRB 070201 having its masses in the range  $1M_\odot < m_1 < 3M_\odot$  and  $1M_\odot < m_2 < 40M_\odot$  to be located in the spiral arm of the Andromeda galaxy [5]. This conclusion was reached by analyzing the LIGO data, associated with the science run S5, lasting around 180 seconds around the time of the GRB 070201. Interestingly, the LSC employed the 2PN-accurate TaylorF2 templates to filter the LIGO data while searching for inspiral GWs from non-spinning compact binaries in the above mass range [34]. It is astrophysically quite possible that the above progenitor candidate will have some tiny non-zero residual orbital eccentricity and therefore, we explored the ability of the 2PN-accurate TaylorT4 approximant to extract the inspiral GWs from compact binaries having residual initial  $e_t \sim 10^{-3}$ . The use of the 2PN-accurate TaylorT4 approximant is justified as the 2PN-accurate TaylorF2 templates are only the analytical Fourier-domain version of the time-domain TaylorT4 templates. The numbers listed in Table VI indicate that the TaylorT4 approximant is effectual with respect to our eccentric GW signal only in the high total mass scenario like the case involving  $m_1 = 3M_\odot$ ,  $m_2 = 40M_\odot$  and in these cases the search templates are highly unfaithful. For other mass combinations, the TaylorT4 templates are neither effectual nor faithful. The entries listed in Table VI force us to state that further investigations involving the relevant LIGO data sets and the various PN-accurate LAL templates would be very useful to clarify the real implications of our FF results. Finally, we would like to state that the above detailed FF experiments were repeated several times by employing a wide range of initial values for  $m$  and  $\eta$ , required by the *amoeba* routine, and the numbers listed in our tables belong to the runs that provided the best possible FFs.

The results arising from our various numerical experiments force us to conclude that it is rather desirable (and may be urgent) to explore the ability of various  $x$ -based PN-accurate inspiral templates, prescribed in Refs. [4, 12], to capture inspiral GW signals from astrophysical compact binaries that are bound to have tiny residual orbital eccentricities.

#### IV. CONCLUSIONS

In this paper, we probed the ability of a number of traditional PN-accurate circular inspiral templates, based

on the adiabatic TaylorT1, completely adiabatic TaylorT1 and adiabatic TaylorT4 approximants, to capture inspiral GWs from compact binaries having tiny residual orbital eccentricities. Our inspiral GW signals are modeled by adapting the phasing formalism of Ref. [10] and therefore originate from compact binaries moving in 3PN-accurate eccentric orbits, specified by  $\xi$  and  $e_t$ , that are perturbed by the 2PN-accurate RR effects. We demonstrate that the traditional circular templates that incorporate 2PN-accurate RR effects are neither effectual nor faithful in capturing our GW signals having tiny orbital eccentricities. However, PN-accurate circular templates based on the recently introduced TaylorEt approximant are both effectual and faithful with respect to GW signals having small orbital eccentricities like 0.1. We explained the physical motivation for employing  $\xi$ , a measure of the instantaneous orbital binding energy, to describe PN-accurate circular and eccentric orbits. With the help of a number of FF experiments, we explored the implications of using only the traditional PN-accurate inspiral templates to filter the LIGO data.

We are planning and pursuing a number investigations motivated by the physical, numerical relativity and data analysis considerations to probe various aspects of the

TaylorEt approximant, both circular and eccentric. It will be desirable to extend the present study by including at least the 3PN-accurate RR effects in an accurate and efficient manner and which include the  $\tilde{e}_\alpha$  contributions while describing the inspiral dynamics of PN-accurate eccentric binaries, relevant for both the ground-based and the proposed space-based GW interferometers. Using such a PN-accurate dynamics, it will be interesting to reexamine what is pursued in Ref. [25], while employing  $\xi$  rather than  $\omega \equiv \langle \frac{d\phi}{dt} \rangle$  to describe the PN-accurate orbit. We are in the middle of incorporating the spin effects into the present study with the help of inputs that generalize what is detailed in Ref. [35].

### Acknowledgments

It is our pleasure to thank Gerhard Schäfer for helpful discussions and persistent encouragement. This work is supported in part by DFG's SFB/TR 7 "Gravitational Wave Astronomy" and DLR (Deutsches Zentrum für Luft- und Raumfahrt).

- 
- [1] Following URLs provide detailed information about the operational GW interferometers: <http://www.ligo.caltech.edu>, <http://www.virgo.infn.it>, <http://www.geo600.uni-hannover.de>, and <http://tamago.mtk.nao.ac.jp>.
  - [2] C. W. Helstrom, *Statistical Theory of Signal Detection*, 2nd ed. (Pergamon Press, London, 1968).
  - [3] Information about the LIGO Scientific Collaboration can be found at <http://ligo.org/>.
  - [4] T. Damour, B. R. Iyer and B. S. Sathyaprakash, Phys. Rev. D **63** (2001) 044023 [Erratum-ibid. D **72** (2005) 029902] [arXiv:gr-qc/0010009].
  - [5] LIGO Scientific Collaboration and K. Hurley, arXiv:0711.1163v2 [astro-ph].
  - [6] P.C. Peters, Phys. Rev. **136**, B1224 (1964).
  - [7] K. Martel and E. Poisson, Phys. Rev. D **60**, 124008 (1999).
  - [8] M. Tessmer and A. Gopakumar, Phys. Rev. D **78**, 084029 (2008) [arXiv:0712.3199 [gr-qc]].
  - [9] P. Ajith, B. R. Iyer, C. A. K. Robinson and B. S. Sathyaprakash, Phys. Rev. D **71**, 044029 (2005) [Erratum-ibid. D **72**, 049902 (2005)] [arXiv:gr-qc/0412033].
  - [10] T. Damour, A. Gopakumar, and B. R. Iyer, Phys. Rev. D **70**, 064028 (2004).
  - [11] A. Gopakumar, arXiv:0712.3236 [gr-qc].
  - [12] M. Boyle *et al.*, Phys. Rev. D **76**, 124038 (2007) [arXiv:0710.0158 [gr-qc]].
  - [13] R.-M. Memmesheimer, A. Gopakumar, and G. Schäfer, Phys. Rev. D **70**, 104011 (2004).
  - [14] T. Damour, B. R. Iyer and B. S. Sathyaprakash, Phys. Rev. D **57**, 885 (1998) [arXiv:gr-qc/9708034].
  - [15] C. Königsdörffer and A. Gopakumar, Phys. Rev. D **73**, 124012 (2006).
  - [16] M. Tessmer and A. Gopakumar, Mon. Not. Roy. Astron. Soc. **374**, 721 (2007) [arXiv:gr-qc/0610139].
  - [17] T. Damour and G. Schäfer, Nuovo Cimento Soc. Ital. Fis., B **101**, 127 (1988).
  - [18] L. Blanchet, "Gravitational Radiation from Post-Newtonian Sources and Inspiralling Compact Binaries", Living Rev. Relativity **5**, (2002): <http://www.livingreviews.org/lrr-2002-3>
  - [19] L. Blanchet and G. Schäfer, Class. Quant. Grav. **10**, 2699 (1993).
  - [20] R. Rieth and G. Schäfer, Class. Quant. Grav. **14**, 2357 (1997).
  - [21] A. Gopakumar and B. R. Iyer, Phys. Rev. D **56**, 7708 (1997).
  - [22] S. Mikkola, *Celestial Mechanics*, **40**, 329 - 334, (1987).
  - [23] L. Blanchet and G. Schäfer, Mon. Not. R. Astron. Soc. **239**, 845 (1989).
  - [24] K. G. Arun, L. Blanchet, B. R. Iyer and M. S. S. Quisailah, arXiv:0711.0250 [gr-qc]; *ibid* arXiv:0711.0302 [gr-qc].
  - [25] I. Hinder, F. Herrmann, P. Laguna and D. Shoemaker, arXiv:0806.1037 [gr-qc].
  - [26] A. Gopakumar, M. Hannam, S. Husa and B. Bruegmann, Phys. Rev. D **78**, 104007 (2008) [arXiv:0712.3737 [gr-qc]].
  - [27] T. Damour, P. Jaranowski and G. Schäfer, Phys. Lett. B **513**, 147 (2001) and references therein.
  - [28] L. Blanchet, T. Damour, B. R. Iyer, C. M. Will, and A. G. Wiseman, Phys. Rev. Lett. **74**, 3515 (1995); L. Blanchet, T. Damour, and B. R. Iyer, Phys. Rev. D **51**, 5360 (1995); C. M. Will and A. G. Wiseman, Phys.



- Rev. D **54**, 4813 (1996).
- [29] K.S. Thorne in *300 years of gravity*, edited by S.W. Hawking and W. Israel (Cambridge University Press, Cambridge, England, 1987) 330; C. M. Bender and S. A. Orszag, *Advanced Mathematical Methods for Scientists and Engineers*, (McGraw Hill, Singapore, 1984).
- [30] Details about the LSC algorithm library (LAL) may be found at <http://www.lsc-group.phys.uwm.edu/lal>.
- [31] W. H. Press, W. T. Vetterling, S. A. Teukolsky and B. P. Flannery, *Numerical Recipes in C++: the art of scientific computing*, Cambridge University Press, (2002).
- [32] B. J. Owen, Phys. Rev. D **53**, 6749 (1996) [arXiv:gr-qc/9511032].
- [33] S. Bose, A. Gopakumar and M. Tessmer, arXiv:0807.2400 [gr-qc].
- [34] P. Brady and N. Fotopoulos, private communication.
- [35] M. Hannam, S. Husa, B. Brügmann and A. Gopakumar, Phys. Rev. D **78**, 104007 (2008) [arXiv:0712.3787 [gr-qc]].

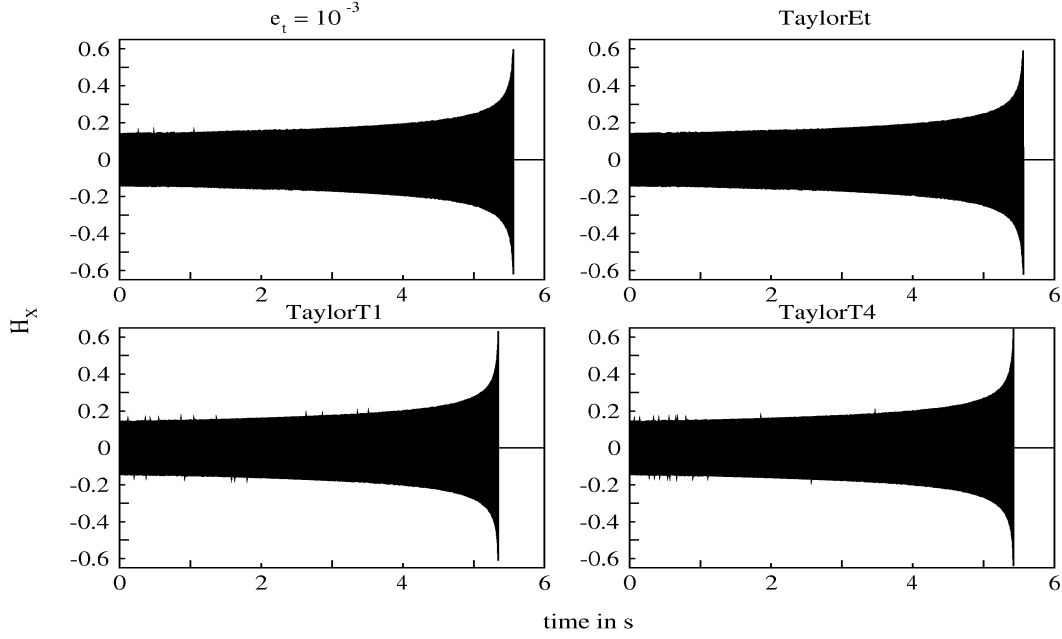


FIG. 1: A set of plots that display the temporal evolution for  $H_{\times}(t) = h_{\times}|_Q(t) / (\frac{Gm\eta C}{R'c^2})$ , originating from a neutron star-black hole binary having  $m_1 = 10 M_{\odot}$  and  $m_2 = 1.4 M_{\odot}$ , and in the initial LIGO frequency window. The top left panel depicts an eccentric orbital evolution of Sec. II, having an initial orbital  $e_t = 10^{-3}$ . The other three plots are for the circular templates modeled after the TaylorEt approximant, the adiabatic TaylorT1 and T4 approximants and these are given by Eqs. (18), (15) and (17), respectively. The accumulated number of GW cycles in the initial LIGO frequency window, defined by  $40\text{Hz} - (6^{3/2} G m \pi / c^3)^{-1} \text{ Hz}$ , are  $\sim 346.264, 346.257, 326.048, 333.622$  for the eccentric inspiral and circular inspirals defined by the TaylorEt, adiabatic TaylorT1 and T4 approximants, respectively.



TABLE I: The initial LIGO FFs involving the 2PN-accurate circular TaylorT4 approximant for the three types of canonical binaries. The fiducial GW signals from compact binaries in inspiralling eccentric orbits are constructed using the phasing formalism detailed in Sec. II. The templates that provide the listed fully maximized minimax-overlap (FF) are characterized by  $m_t$  and  $\eta_t$ . In the case of double neutron-star binaries, we terminate the the temporal evolution of both the GW signal and circular templates when their respective GW frequencies reach 1000Hz. In the  $e_t \equiv 0$  cases, we employ the TaylorEt approximant to model the fiducial GW signals and the associated numbers can be considered to represent what to expect for initial  $e_t < 10^{-3}$ . The numbers indicate that the 2PN-accurate TaylorT4 templates are neither effectual nor faithful while dealing with inspiral GWs from compact binaries having tiny orbital eccentricities.

$m_1/M_\odot : m_2/M_\odot$		1.4 : 1.4	1.4 : 10.0	10.0 : 10.0
$e_t \equiv 0$	FF	0.822	0.939	0.957
	$m_t$	2.800	6.906	19.04
	$\eta_t$	0.248	0.250	0.247
$e_t = 0.001$	FF	0.821	0.939	0.951
	$m_t$	2.800	6.906	20.00
	$\eta_t$	0.248	0.250	0.224
$e_t = 0.01$	FF	0.821	0.938	0.951
	$m_t$	2.800	6.909	20.00
	$\eta_t$	0.248	0.250	0.225
$e_t = 0.10$	FF	0.708	0.830	0.830
	$m_t$	2.800	6.943	19.00
	$\eta_t$	0.250	0.250	0.250

TABLE II: Values of the FFs and the associated biases in  $m$  and  $\eta$  values, while employing the circular inspiral templates based on the adiabatic T1 and the complete adiabatic T1 approximants. The complete adiabatic TaylorT1 templates are employed to incorporate the effects of 3PN-accurate conservative dynamics into the  $x$ -based circular templates [9]. The conclusions and other details are similar to what is observed in Table I.

$m_1/M_\odot : m_2/M_\odot$		1.4 : 1.4	1.4 : 10.0	10.0 : 10.0
Standard adiabatic TaylorT1 templates				
$e_t \equiv 0$	FF	0.771	0.843	0.894
	$m_t$	2.785	6.845	18.55
	$\eta_t$	0.250	0.250	0.243
$e_t = 0.001$	FF	0.768	0.842	0.891
	$m_t$	2.800	6.846	18.57
	$\eta_t$	0.248	0.250	0.242
$e_t = 0.01$	FF	0.766	0.841	0.841
	$m_t$	2.800	6.834	6.837
	$\eta_t$	0.248	0.250	0.250
$e_t = 0.10$	FF	0.677	0.766	0.778
	$m_t$	2.800	6.876	20.01
	$\eta_t$	0.249	0.250	0.216
Complete adiabatic TaylorT1 templates				
$e_t \equiv 0$	FF	0.761	0.800	0.878
	$m_t$	2.783	6.820	18.41
	$\eta_t$	0.250	0.250	0.245
$e_t = 0.001$	FF	0.761	0.800	0.878
	$m_t$	2.786	6.821	18.41
	$\eta_t$	0.250	0.250	0.246
$e_t = 0.01$	FF	0.758	0.800	0.878
	$m_t$	2.800	6.820	18.41
	$\eta_t$	0.247	0.250	0.247
$e_t = 0.10$	FF	0.673	0.754	0.838
	$m_t$	2.800	6.867	18.55
	$\eta_t$	0.249	0.249	0.247

TABLE III: The results of FF computations that employ the circular templates based on the TaylorEt approximant. It is important to note that the temporal evolution for both the eccentric GW signals and the circular templates require the 3PN accurate conservative and the 2PN-accurate reactive dynamics. The rest of the details are as in Tables I and II. The displayed values clearly demonstrate, not surprisingly, that the circular TaylorEt templates are both effectual and faithful with respect to our inspiral GW signals having tiny orbital eccentricities.

$m_1/M_\odot : m_2/M_\odot$		1.4 : 1.4	1.4 : 10.0	10.0 : 10.0
$e_t = 0.001$	FF	0.999	1.000	1.000
	$m_t$	2.824	11.50	20.17
	$\eta_t$	0.246	0.106	0.246
$e_t = 0.010$	FF	0.999	1.000	1.000
	$m_t$	2.823	11.45	20.18
	$\eta_t$	0.247	0.107	0.246
$e_t = 0.100$	FF	0.804	0.921	0.956
	$m_t$	2.811	11.44	20.20
	$\eta_t$	0.250	0.108	0.249

TABLE IV: The initial LIGO FFs involving GW signals modeled after the circular TaylorEt approximant and the circular templates based on the TaylorT4 approximant, both requiring 2.5PN-accurate reactive dynamics. The TaylorEt GW signals are constructed using the 3PN-accurate expression for  $d\phi/dt$  and the 2.5PN-accurate expression for  $d\xi/dt$ , while the TaylorT4 approximant requires the 2.5PN-accurate expression for  $dx/dt$ . These PN-accurate expressions are extractable from Eqs. (6) and (7) in Ref. [33]. We conclude that for low mass binaries, the TaylorT4 approximant is not very effectual and in the case of high  $m$  binaries, the circular templates are fairly unfaithful.

$m_1 : m_2$	FF	$m_t$	$\eta_t$
5-5	0.933	9.900	0.250
3-9	0.868	9.888	0.248
3-12	0.897	11.26	0.249
5-10:	0.903	13.47	0.250
5-15:	0.937	16.20	0.249
10-10	0.995	20.51	0.232
15-15	0.995	30.72	0.231

TABLE V: The results originating from one of our FF experiments motivated by the Fig. 4 in Ref. [26]. The inspiral GW signals are based on the circular TaylorEt approximant, given by Eq. (7) in Ref. [33] and therefore specified by the 3PN-accurate expression for  $d\phi/dt$  and the 3.5PN-accurate expression for  $d\xi/dt$ . The circular templates are given by the 2PN-accurate TaylorT4 approximant. Somewhat higher FFs are observed only for high mass binaries with  $m \geq 30 M_\odot$ .

$m_1/M_\odot : m_2/M_\odot$	FF	$m_t$	$\eta_t$
5-5	0.849	9.744	0.247
1.4-10	0.877	6.891	0.250
3-9	0.868	9.871	0.248
3-12	0.858	14.058	0.163
10-10	0.942	18.940	0.247
15-15	0.971	27.701	0.241

TABLE VI: The initial LIGO FF values in the mass range relevant for the GRB 070201 progenitor following Ref. [5]. The fiducial inspiral GW signals are from compact binaries having initial  $e_t = 10^{-3}$  and computed using the phasing formalism of Sec. II. The value of  $e_t$  can be treated to be representative of still lower residual initial eccentricities and the circular templates are based on the 2PN-accurate TaylorT4 approximant. Even though, the employed circular templates are neither effectual nor faithful for several mass combinations, we reiterate that further investigations involving the relevant LIGO data should be useful to make any physical implications of our ideal FF experiments.

$m_1/M_\odot : m_2/M_\odot$	FF	$m_t$	$\eta_t$
3- 1	0.837	3.363	0.250
1-10	0.909	5.702	0.250
3-10	0.876	10.335	0.249
1-20	0.937	7.634	0.250
3-20	0.945	14.029	0.250
1-40	0.966	11.680	0.195
3-40	0.972	20.675	0.208